

6-1997

The effect of protein environment and ring substitution on the electrostatic charges, dipole moment, and ultraviolet spectra of flavin

Jared Berger

Union College - Schenectady, NY

Follow this and additional works at: <https://digitalworks.union.edu/theses>



Part of the [Chemistry Commons](#)

Recommended Citation

Berger, Jared, "The effect of protein environment and ring substitution on the electrostatic charges, dipole moment, and ultraviolet spectra of flavin" (1997). *Honors Theses*. 2057.
<https://digitalworks.union.edu/theses/2057>

This Open Access is brought to you for free and open access by the Student Work at Union | Digital Works. It has been accepted for inclusion in Honors Theses by an authorized administrator of Union | Digital Works. For more information, please contact digitalworks@union.edu.

UN
X
2
3
4
5
6
7

**The Effect of Protein Environment and
Ring Substitution on the Electrostatic Charges,
Dipole Moment, and Ultraviolet Spectra
of Flavin**

Jared Berger
Chemistry
1997

1997
2
3
4
5
6
7

Table of Contents:

Table of Contents	p. i
Table of Contents: Tables	p. ii
Table of Contents: Figures	p. iii
Abstract	p. 1
Acknowledgement	p. 2
Introduction	p. 3-6
Procedure	p. 7-8
Explicit Directions for Using Spartan	p. 8-9
Results	p. 10-13
Discussion	p. 14-16
Appendix: Figures	p. I-XIII
Appendix: Work Cited	p. XIV

Table of Contents: Tables

Table 1: Corrections to PDB Structure for Flavin Using Macromodel	p. 7
Table 2: Constrained Distances From Flavin to Overlay Molecules Used in Spartan	p. 8
Table 3: Dipole Moment for FMN, 8-Azido-FMN, and 6-Sulfoxo-FMN	p. 10
Table 4: Electrostatic Charges for FMN Outside and Inside the Protein Environment	p. 11
Table 5: Electrostatic Charges for 8-Azido-FMN Outside and Inside the Protein Environment	p. 11
Table 6: Electrostatic Charges for 6-Sulfoxo-FMN Outside and Inside the Protein Environment	p. 12
Table 7: Ultraviolet Absorption Wavelengths for FMN, 8-Azido-FMN, and 6-Sulfoxo-FMN	p. 13

Table of Contents: Figures

Figure 1: Old Yellow Enzyme - Wireframe	p. I
Figure 2: Old Yellow Enzyme - Ribbons	p. II
Figure 3: Complete Structure of the Flavin	p. III
Figure 4: Modified Flavin Used in Spartan	p. IV
Figure 5: Modified Flavin Within the Protein Environment Used in Spartan	p. IV
Figure 6: Modified 8-Azido-FMN Used in Spartan	p. V
Figure 7: Modified 6-Sulfoxo-FMN Used in Spartan	p. V
Figure 8: Dipole Moment of FMN Outside and Inside Protein Environment	p. VI
Figure 9: Dipole Moment of 8-Azido-FMN Outside and Inside Protein Environment	p. VII
Figure 10: Dipole Moment of 6-Sulfoxo-FMN Outside and Inside Protein Environment	p. VIII
Figure 11: Major Changes in the Electrostatic Charges for FMN, 8-Azido-FMN, and 6-Sulfoxo-FMN	p. IX
Figure 12: Some of the Possible Resonance Structures for FMN	p. X
Figure 13: Some of the Possible Resonance Structures for 8-Azido-FMN	p. XI
Figure 14: Some of the Possible Resonance Structures for 6-Sulfoxo-FMN	p. XII
Figure 15: Sideview of FMN Outside and Inside the Protein Environment	p. XIII

Abstract:

Old Yellow Enzyme is an interesting protein due to its involvement in many biochemical systems, such as bioluminescence and degradation of variety of substrates. The flavin mononucleotide (FMN) is the active site of the protein. The FMN is an isoalloxazine ring with a phospholipid tail, which attaches to the protein through a phosphate group and hydrogen bonding in the hydrophilic section of the ring system. My research is a theoretical, computational calculation, which uses Spartan, a quantum mechanical calculation program, to determine how the dipole moment and electrostatic charges change upon the substitution of the FMN and within the protein environment. The geometry optimization of flavin used AM1 and MNDO which are both semi-empirical quantum mechanical programs. After optimization, the dipole moment and the electrostatic charges were calculated. The same steps were executed for the flavin within the protein environment. 8-azido-FMN and 6-sulfoxo-FMN were also studied to determine the effect of ring substitution on charge distribution. Before the calculations could be performed, the flavin and the protein environment had to be modified. The phospholipid tail of the flavin was replaced by a methyl group. The protein itself was modeled by "overlay" protein molecules which are close to flavin in the crystal structure. These overlay molecules were placed in the same orientation as found in the real protein and constrained to known distances from the ring system. All of these modifications are presumed not to affect the calculations since no π electrons were removed from the flavin or the protein. The evidence collected showed that the dipole moment of flavin significantly changed when placed in a "protein" environment. The electrostatic charges also changed upon placement into the "protein" environment. Upon comparing the changes in the electrostatic charge to the resonance structures of the flavin, the positive and negative charges occurred on the same atoms that have a positive or negative charge in the resonance structures. This pattern supports the theory that the flavin is stabilized by two or more resonance structures within the protein.

Acknowledgment:

I would like to thank Professor Anderson for her guidance and help, especially with learning about Spartan and dealing with the Silicon Graphic computer. I would also like to thank Professor Fox for asking a question I could answer with my research. She also gave me some needed information about Old Yellow Enzyme such as the crystal structure of the flavin and the hydrogen bond attachment.

Introduction:

The Old Yellow Enzyme (Figure 1 & 2) was first isolated in 1932 from brewer's yeast by Warburg and Christian (Schopfer p. 248). OYE is involved in many biological systems: degradation of variety of substrates, one-electron transport process, activation of molecular oxygen, bioluminescence, photochemical processes (i.e. phototropism), and probably in the control of the enzymatic functions.

Old Yellow Enzyme has an overall structure of 399 residues folded into a single domain of a parallel, eight-stranded α/β barrel. The flavin phosphoryl group is bound to the amino terminus of helix D, which is between the $\beta 8$ and helix 8 strands. The flavin mononucleotide (FMN) (Figure 3), which is an isoalloxazine ring, is attached to the protein through a phosphate group (Fox p. 1091). The isoalloxazine ring is amphipathic, which means it has a hydrophobic region and a hydrophilic region. The hydrophobic region of the ring or the *re*-face of the flavin is buried within carboxy-terminal loops, which inhibits the accessibility the solvent to the interior of the barrel. However, the *re*-face is buried near the strand $\beta 1$, which has hydrogen bonding between the protein and the ribityl phosphate moieties. The *si*-face is active site of the pocket and is exposed to the solvent. Thus, the *si*-face is the hydrophilic region of the isoalloxazine ring. The FMN, at carbon 7 and 8, has a dimethylbenzene edge, which is loosely surrounded by aromatic side chains of phenylalanine (Phe) 296, Phe 374, and tyrosine (Tyr) 375. This dimethylbenzene edge has some mobility, which allows the flavin access to the solvent (Fox p. 1093).

The structure described above is for the oxidized state of the flavin protein; however, the two other states, semiquinone and reduced state, have different characteristics. For example, the reduced state is electron rich, while the oxidized state is electron-poor. The first change for the reduced state is the replacement of a bound chloride ion with two ordered molecules of water in the FMN-binding site. One of these two ordered water molecules interacts with histidine (His) 191 and asparagine (Asn) 914 of the protein. A second water molecule interacts with the first water molecule and is properly

positioned to accept a hydrogen bond from the protonated N_5 atom of the FMN. A fifteen percent butterfly bending of the ring occurs with the puckering found at N_5 atom of the flavin, which is involved in the movement of the dimethylbenzyl portion. The C_5' atom of the FMN ribityl group moves 1.6 angstroms and switches from one staggered form to another staggered form (Fox p. 1100).

In the transformation from the oxidized state to the reduced state, each atom of the flavin binding site, which can be seen in Figure 3, goes through its own transformation depending on its accessibility to the solvent, presence of a reactive amino acid side chain, electrostatic environment, and steric constraints (Schopfer p. 257). The C_8 , which lacks steric hindrance, undergoes conformational change upon binding of a ligand. When this position is halogenated, it is susceptible to nucleophilic displacement, especially by thiols. Therefore, this position is known to be accessible to the solvent. However, when pentafluorophenol, and α -O²⁵-6Beta-cyclo 1,4,5,6 tetrahydro NADP were added, the nucleophilic displacement was effectively inhibited, which suggested no steric hindrance (Schopfer p. 258). At C_2 , a nearby positive charge or hydrogen bond between C_2 and an oxygen was indicated by ¹³C NMR studies. This characteristic explains the formation of an anionic reduced form of native OYE and the formation of a stable anionic semiquinone. However, the C_2 position generally experiences a hydrophobic environment (Schopfer p. 260). The C_6 is surrounded by a positively charged protein residue. The evidence comes from the photochemistry of 6-azido-FMN OYE. N_5 has a positive charge as indicated by ¹³C NMR study. An unlikely interpretation would be a hydrogen bond to the N_5 , because of its low pKa (Schopfer p. 260). The C_4 has access to the solvent because of its reactivity to peroxide. When pentafluorophenol is bound to 4-thio-FMN OYE, the reaction rate with the peroxide is decreased. This slower reaction rate indicated that significant conformational change occurred upon a ligand binding (Schopfer p. 261). The N_1 position is hydrogen bonded in the native or oxidized state of OYE. This bond suggests a closer

contact between the oxidized state of the protein and the flavin than between the reduced state of the flavin (Schopfer p. 261).

Taking into consideration all of the above data, the following summary can be compiled. From position 8 to position 4, the isalloxazine ring has access to the solvent and is hydrophilic. The other side of the ring is hydrophobic and is protected from the solvent. Positive charges, near the N_3-C_2 and C_6-N_5 , are strong enough to attract negative charged ligands. The protein is connected to the flavin through hydrogen bonding at $C_4=O$ and N_5 -protein (Schopfer p. 261).

The structure of the flavin allows for the binding a wide variety of structurally diverse ligands such as simple inorganic and organic anions, aromatic hydrocarbons (especially phenolate anions), to pyridine nucleotide derivatives (Schopfer p. 252). The most interesting of the ligands are the phenolic compounds. For example, *p*-hydroxybenzaldehyde (PHB) is responsible for the green form of the OYE. Thiophenol with some condensed compounds contain hydroxyl moieties which cause the appearance of long wavelength absorbance bands. Aromatic compounds, without the hydroxyl moiety, did not cause this long wavelength band. The phenol ring displaces the chloride ion within the active site. The ring lies above the *si*-face of the flavin ring with the two planes lying parallel to each other (Fox p.1094). The newly formed hydrogen bonds which hold the phenol ring to the protein are linear and strong (Fox p.1097-8).

Using PHB as an example, the changes in the flavin and the protein can be seen. When PHB binds, the hydroxyl of Tyr 375 moves 2 angstroms in order to be in a better position for hydrogen bonding. Phe 296 and Phe 250 undergo minor adjustments in their conformation. His 191 and Asn 194, which act as hydrogen bond donors, form a hydrogen bond with the ionized phenolate oxygen (Fox p.1097-8). Some other changes deal with the movement of the flavin, which is essential for the translation of substrates and products into a more solvent-shielded active site during a catalysis reaction. The isalloxazine ring moves away from the substrate and into the solvent, which increases the

accessibility of the flavin to the solvent. This adjustment can be seen in the changes of the electron density (Galfi p. 110). The structure, after the binding, involves a charge transfer interaction with a close physical association of the flavin and the PHB. The closeness stems from the sharing of electrons between the π electrons of the phenolic ring with the pi electrons of the flavin ring. The distance between the phenolate oxygen and the flavin atom C₂ is 3.0 angstroms, while the distance between the C₁ of the PHB atom and the N₃ of the flavin are 3.4 angstroms. These distances demonstrate the closeness of the flavin and the PHB. However, this new structure does not affect the interactions between the protein and the flavin (Fox p.1097-8). The binding of the ligands has shown to be depended on the pH, in experiments using p-chlorophenol and pentafluorophenol. These ligands bind differently depending on the pH of the solvent (Abramovitz p. 5332).

Procedure:

The first step is to download the X-Ray coordinates of the oxidized and reduced flavin protein from the Brookhaven Protein Data Bank using the internet. The file is opened as a text file and the 126 water molecules at the end of the file are deleted. The file is saved as `pdbblyl.ent` and then altered to correct the structure of the flavin protein for the Macromodel program (Fox p. 1095). The changes which need to be made to the flavin are in Table 1.

Table 1: The corrections to the PDB structure required to allow the flavin moiety to be used correctly in Macromodel.

atom	original version	corrected version
3179	29 3180 1 3196 1	25 3180 1 3196 2
3185	5 3183 1 3186 1	2 3183 1 3186 2 3196 1
3186	34 3185 1 3187 1	25 3185 2 3187 1
3187	4 3186 1 3188 1 3194 1	2 3186 1 3188 1 3194 2
3188	5 3187 1 3189 1	7 3187 1 3189 2
3189	4 3188 1 3190 1 3191 1	2 3188 2 3190 1 3191 1
3191	4 3189 1 3192 1 3193 1	2 3189 1 3192 1 3193 2
3193	5 3191 1 3194 1	7 3191 2 3194 1
3194	4 3187 1 3193 1 3195 1	2 3187 2 3193 1 3195 1
3195	33 3194 1 3196 1 3197 1	25 3194 1 3196 1 3197 1
3196	5 3179 1 3195 1	2 3179 2 3195 1 3185 1
3207	17 3206 1	18 3206 1
3208	17 3206 1	15 3206 2
3209	17 3206 1	18 3206 1

The corrected file will allow for the determination of the location of the protein attaching molecules to the flavin protein.

Using Spartan, an abbreviated flavin molecule was constructed as seen in Figure 4. The phospholipid tail was replaced with a methyl group to decrease the number of atoms. The flavin was altered because Spartan is unable to handle a large number of atoms easily. After the structure was successfully constructed, its geometry was optimized using the AM1 and MNDO semi-empirical quantum mechanical programs in Spartan. When the optimization is complete, Spartan is used to determine the dipole moment and electrostatic charges, and the UV absorbance spectrum. Running all the tasks at once tended to overload the system, therefore, was submitted as a separate job. The modifications, which

were made to flavin, were presumed not to affect the calculations since only the aliphatic phospholipid tail was removed, leaving the π electrons undisturbed.

The next step is to determine how to model the OYE protein interaction with flavin. Methyl groups can be substituted for aliphatic, nonpolar regions of the protein. The protein regions of T37, G72, Q114, and R243 were modified and placed in the correct orientation surrounding the flavin as seen in Figure 5. The distances, which are the same distances as for hydrogen bonds in the crystal structure of OYE, are used to constrain the overlay molecules to the flavin. The values used are Table 2.

Table 2: The Constrained Distances Used In Spartan From the Flavin to the Overlay Molecules For the Hydrogen Bonding

Flavin Atom	Overlay Molecule Atom	Distance (Angstroms)
N5	N of Threonine 37	2.91
O4a	O of Threonine 37	2.77
O4a	N of Glycine 72	3.46
N3	O of Glutamine 114	2.85
O2a	N of Glutamine 114	2.99
N1	N of Arginine 243	2.87
N1	N of Arginine 243	2.90

After the modified flavin within the protein model has been created, semi-empirical runs were submitted to optimize the geometry and to determine the dipole moment, the electrostatic charges, and the UV absorption spectrum of the flavin within the protein environment.

The flavin structure was then altered to form both the 8-azido-FMN and the 6-sulfoxo-FMN as seen in Figures 6 and 7. These two flavins were run through the same procedure as the original flavin, both with and without the protein environment. However, all of these calculations were done using the MNDO parameters because the 8-Azido-FMN and the 6-Sulfoxo-FMN would not optimize with the AM1 parameters.

Explicit directions for using Spartan:

The following commands can be found under the heading **Set Up**. Under **Properties**, click on the boxes before the dipole and electrostatic charges. The boxes will turn yellow which indicates that the calculations will be performed. The rest of the options

should be turned off. To obtain UV absorbance wavelengths, under **Semi-Empirical**, type CI in the options box. To change the calculation from geometry optimization to single point calculation, click on the box that contains the words "geometry optimization" and drag over the words "single point calculations". A single point calculation can be used if the geometry optimization has already been performed. Under **Surfaces and Volumes**, no tasks should be contained in the large box. If a task is present, simply click on the task to highlight it and click on the delete square. To run the job, open the **Set Up** and drag down to **Submit**. If the optimization runs out of cycles, click on the restart button under **Semi-Empirical**. Click on the box before the Hessian. Then re-submit the job, by opening the **Set Up** menu and dragging down to **Submit**. This procedure will continue to optimize the structure.

The results of the calculations can be viewed under **Output** found in the **Display** menu. The output data will show the optimization cycles, dipole moment, electrostatic charges, and ultraviolet wavelengths. To view just the dipole moment, highlight **Dipole** under **Properties** under **Display**. This command will show the dipole moment components for the x, y, and z planes as well as the total dipole moment. To exit, hit the period button on the keyboard. To view just the electrostatic charges, highlight the word **Charge** found directly below the word **Dipole**. Click on any atom to view the charge on the individual atom. To view another atom, simply click on a different atom. To exit, hit the period button on the keyboard.

Results:

The dipole moments can be seen in Figure 8 through 10. The yellow arrow represents the dipole moment vector pointing from positive toward negative. Each dipole points toward the hydrophilic or the right side of the ring system, except for the 6-sulfoxo-FMN within the protein environment which points in the opposite direction. The dipole moments are shown in Table 3.

Table 3: The X, Y, and Z Components and Total Dipole Moment for FMN, 8-Azido-FMN, and 6-Sulfoxo-FMN Outside and Inside the Protein Environment for the AM1 and MNDO parameters

model	compound	X components	Y components	Z components	total dipole
AM1	FMN	8.0065	-0.0816	-2.3695	8.3502
MNDO	FMN	6.8546	0.4198	-2.0212	7.1587
AM1	FMN & protein	1.8111	4.9546	1.3430	5.4435
MNDO	FMN & protein	1.7416	-0.0489	-3.8839	4.2567
MNDO	8-Azido-FMN	2.2439	-0.7230	6.5075	6.9214
MNDO	8-Azido-FMN & protein	13.7194	3.2996	-7.8081	16.1268
MNDO	6-Sulfate-FMN	-8.8411	2.0677	3.6007	9.7675
MNDO	6-Sulfate-FMN & protein	4.0730	-5.6908	1.3665	7.1304

As seen in the Table and the Figures, the dipole moment significantly changes upon placement into the protein environment. However, changes for the three flavins do not follow a single pattern. The change in the dipole moment indicated that the π electrons move when the flavin was added to the model protein environment.

The electrostatic charges for the three different flavins are given in Tables 4,5, and

6.

Table 4: The Electrostatic Charges for FMN Outside and Inside the Protein Environment for AM1 and MNDO Parameters. Δq Represents the Change in the Electrostatic Charge When the Flavin Was Added to the Protein Environment

Model		AM1	MNDO	AM1	MNDO	AM1	MNDO
Brookhaven	Spartan	FMN	FMN	FMN & Protein	FMN & Protein	Δq	Δq
C9	C2	-0.07	-0.05	-0.20	-0.08	-0.13	-0.03
C6	C3	-0.39	-0.16	-0.24	-0.08	0.15	0.08
C9A	C4	-0.18	-0.06	-0.03	0.02	0.15	0.08
C8	C5	-0.10	-0.07	0.01	-0.03	0.11	0.04
C7	C6	0.15	-0.00	0.01	-0.04	-0.14	-0.04
C5A	C7	0.52	0.41	0.37	0.27	-0.15	-0.14
N10	N8	-0.08	-0.19	-0.08	-0.22	0.00	-0.03
C8M	C9	-0.17	0.10	-0.17	0.10	0.00	0.00
C7M	C10	-0.19	0.09	-0.15	0.09	0.04	0.00
N5	N11	-0.47	-0.48	-0.38	-0.46	0.09	0.02
C11	C13	0.04	0.18	-0.06	0.13	-0.10	-0.05
C10A	C14	0.37	0.54	0.41	0.50	0.04	-0.04
N1	N15	-0.66	-0.80	-0.67	-0.70	-0.01	0.10
C2	C22	0.86	1.07	0.86	0.96	0.00	-0.11
C4A	C23	0.11	0.03	0.05	0.14	-0.06	0.11
C4	C24	0.64	0.83	0.86	0.71	0.22	-0.12
N3	N25	-0.67	-0.83	-0.74	-0.73	-0.07	0.10
O2A	O26	-0.52	-0.56	-0.52	-0.56	0.00	0.00
O4A	O27	-0.47	-0.52	-0.60	-0.52	-0.13	0.00

Table 5: The Electrostatic Charges for 8-Azido-FMN Outside and Inside the Protein Environment for MNDO Parameter. Δq Represents the Change in the Electrostatic Charge When the Flavin Was Added to the Protein Environment

Brookhaven	Spartan	8-Azido-FMN	8-Azido-FMN & protein	Δq
N5	N1	-0.47	-0.48	-0.01
C5A	C2	0.36	0.29	0.07
C7	C3	-0.05	-0.24	-0.19
C9	C4	-0.23	-0.37	-0.14
C8	C5	0.31	0.55	0.24
C9A	C6	-0.02	0.17	0.19
C6	C7	-0.15	-0.07	0.08
N10	N8	-0.16	-0.08	0.08
C8M	N10	0.85	0.72	-0.13
C8M	N11	-0.67	-0.65	0.02
N1	N13	-0.78	-0.66	0.12
C7M	C14	0.12	0.17	0.05
C8M	N18	-0.30	-0.14	0.16
C10A	C19	0.49	0.14	-0.35
C11	C23	0.18	0.13	-0.05
C4A	C24	0.07	0.20	0.13
C4	C25	0.77	0.62	-0.15
O4A	O26	-0.51	-0.54	-0.03
N3	N27	-0.77	-0.34	0.43
O2A	O29	-0.56	-0.60	-0.04
C2	C30	1.03	0.66	-0.37

Table 6: The Electrostatic Charges for the 6-Sulfoxo-FMN Outside and Inside the Protein Environment for MNDO Parameter. Δq Represents the Change in the Electrostatic Charge When the Flavin Was Added to the Protein Environment

Brookhaven	Spartan	6-sulfate-FMN	6-sulfate-FMN & Protein	Δq
C9	C1	-0.31	-0.35	-0.04
C8	C2	0.10	-0.02	-0.12
C7	C3	-0.33	-0.05	0.28
C8M	C4	0.10	0.17	0.07
C6	C5	0.10	0.12	0.02
C7M	C6	0.16	0.03	-0.13
C9A	C13	0.04	0.25	0.21
N5	N15	-0.35	-0.56	-0.21
N10	N16	-0.18	-0.24	-0.06
S5A	S17	0.32	0.46	0.14
C5A	C18	0.27	-0.05	-0.32
O5A	O19	-0.63	-0.70	-0.07
C10A	C20	0.62	0.46	-0.16
C11	C21	0.19	0.23	0.04
C4A	C25	-0.29	0.11	0.40
C2	C26	1.10	0.94	-0.16
N1	N27	-0.90	-0.80	0.10
C4	C28	0.89	0.55	-0.34
N3	N29	-0.82	-0.62	0.20
O4A	O30	-0.58	-0.48	0.10
O2A	O32	-0.66	-0.64	0.02

Δq represents the change in the electrostatic charge when the flavin was introduced into the protein environment. The value of Δq depends on which parameter set is used, AM1 or MNDO. We classified a major positive change in electrostatic charge if it increased by +0.10 and a major negative change if it decreased by -0.10. If one compares the same atom in the three different flavins, none had major changes in the same direction for all three. Figure 11 represents charges in the electrostatic charge, where blue represents a major positive change and red represents a major negative change.

As seen in Table 7, the literature wavelength values did not agree with the calculated wavelength values. There was a shift to longer wavelengths when the flavin was in the protein environment for both AM1 and MNDO parameters.

Table 7: Calculated Wavelength for the UV Absorption Spectra of the FMN, 8-Azido-FMN, and 6-Sulfoxo-FMN With and Without Protein Attachment

	Model	State	Energy	OS	calc. wavelength (nm)
Flavin	AM1				
		4	3.60	4.27	344
		6	3.94	4.93	315
		10	4.57	4.91	271
		12	5.17	4.76	240
		15	5.55	3.77	223
Flavin	MNDO				
		4	3.02	4.13	410
		5	3.32	5.96	373
		8	4.10	4.97	302
		9	4.54	4.13	273
		14	5.09	2.70	244
FMN & Protein	AM1				
		2	3.87	2.25	321
		4	4.95	2.32	251
FMN & Protein	MNDO				
		3	3.57	3.95	347
		5	4.07	4.84	305
		8	5.28	5.09	235
		12	5.98	6.33	207
8-Azido-FMN	MNDO				
		2	1.90	3.50	652
		4	2.49	6.68	498
8-Azido-FMN & Protein	MNDO				
		3	3.53	6.48	352
		4	3.93	8.00	315
6-sulfoxo-FMN	MNDO				
		4	1.88	2.16	659
		11	2.98	2.13	415
6-sulfoxo-FMN & Protein	MNDO				
		4	1.78	2.69	695

In addition to electrostatic charges, structural changes also occurred when the flavin was placed within the protein environment. The planarity of the isoalloxazine ring system was altered, as seen in Figure 12. Flavin without the protein environment is planar. However, flavin within the protein environment has a butterfly orientation or a bending along the axis created by N5 and N10 atoms.

Discussion:

Before the data is analyzed, the advantages of the AM1 parameters over the MNDO parameters will be discussed. According to M.J.S. Dewar and H.S. Rzepa, the MNDO parameters have trouble with molecules with heteroatoms, such as those in the flavin ring. They also showed that the AM1 parameters better reproduce hydrogen bonds than the MNDO parameters. Therefore, the AM1 parameters is the parameter system that should be used. Unfortunately, the 8-Azido-FMN and the 6-Sulfoxo-FMN within the protein environment would not optimize with AM1 parameters. Thus, MNDO parameters were used with the substituted flavins.

One of the main objectives was to determine if the flavin were stabilized within the protein environment by forming resonance structures to delocalize the π -electrons. In Figure 13, some of the possible resonance structures of the flavin are shown. The two starred structures are the ones most likely to occur in the protein environment. As seen in Figure 8, the calculated dipole moment of flavin points from the right to the left which agrees with starred resonance structures. The electrostatic charges, which are seen Figure 11, also support these resonance structures. According to the Brookhaven numbering system, C6 and C7 has a positive charge in both the resonance structures and the electrostatic charge. Therefore, it is concluded that the flavin in the protein is stabilized by resonance structures.

Resonance structures of 8-Azido-FMN as seen in Figure 14 have the positive charge on the right side of the flavin and the negative charge on the left side. The calculated dipole moment in Figure 9 mimics this pattern. The positive major charge at C6 can be found in both the resonance structure and in Figure 11. However, the other charged atoms in the resonance structures are not found in Figure 11. Therefore, it can be concluded that the calculations for 8-Azido-FMN agree somewhat with possible resonance structures. Neither the calculated dipole moment nor the electrostatic charge data agree with the two proposed resonance structures for 6-Sulfoxo-FMN as seen in Figure 15. However, it is

important to note that, for the 8-Azido-FMN and the 6-Sulfoxo-FMN, other resonance structures may be possible.

The calculation of ultraviolet wavelength did not agree with observed values. This may have been due to the protein or flavin modifications and the lack of solvent in the calculations. Although Spartan allows calculations to be done with or without solvent. No solvent was used so that the calculations would finish in a reasonable amount of time.

According to Chirt Moonen, Jacques Vervoort, and Franz Muller, the structure of the free flavin, without the protein environment, and the bound flavin, with the protein environment, are different. The free flavin has a planar structure, while the bound flavin has a "butterfly" bend (Moonen p. 4860). As seen in Figure 15, my research showed that the flavin behaved in the same manner. This similarity in shape indicates that our modified flavin and protein environment may be reasonable approximations to the actual flavin in OYE.

^{13}C NMR studies indicate that O4 α receives electrons from N10. The calculations presented here show no change in the charge of N10 indicating that no electron movement occurred at that atom. This lack of agreement indicates that the modifications of flavin and of the protein environment could have affected the results near the phospholipid tail.

It is clear from these calculations that electrons move when the flavin is placed within a protein environment. However, there are three major limitations which may have affected my calculations. The first limitation deals with the Spartan computer program. Spartan has a limit on the number of atoms that can be used in energy minimization. This atom limitation required modification to the flavin and the protein environment. The second limitation are the parameters used for the 8-Azido-FMN and the 6-Sulfoxo-FMN. AM1 is the better parameter system for the heteroatom flavin. Thus, the first step would be to optimize these substituted ring systems while the flavins are within the protein environment using the AM1 parameters. Hopefully, this step would enhance the accuracy of the calculations. The final limitation deals with the uncertainty of the modifications of the

protein. In order to obtain good results, the modifications should affect the calculations as little as possible, if at all.

Appendix:

Figure 1: Wireframe Picture of Old Yellow Enzyme - Flavin is green and in the middle of the structure.

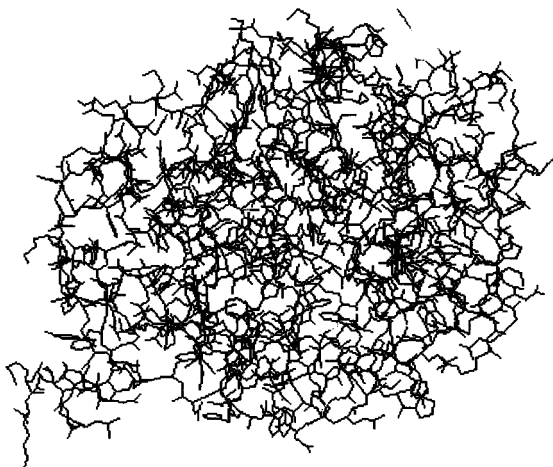


Figure 2: Old Yellow Enzyme - Pink are the alpha helixes. Yellow are the beta pleated sheets. Green is the flavin.

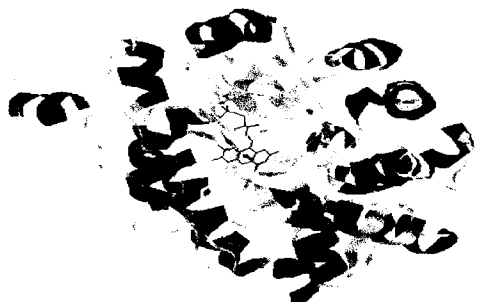


Figure 3: The Full Structure of the Active Site (Flavin) of Old Yellow Enzyme
Red- Oxygen; Blue - Nitrogen; White - Hydrogen; Black - Carbon; Purple - Phosphorous

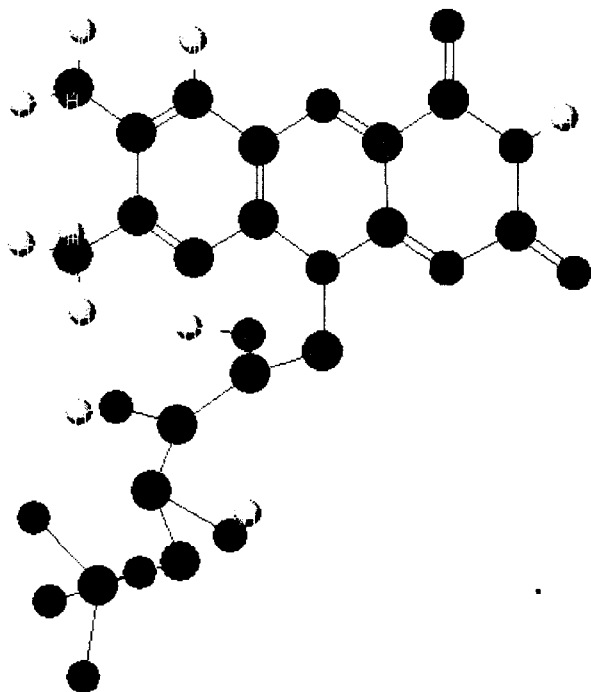


Figure 4: The Modified Version of the Flavin Used in the Spartan Program

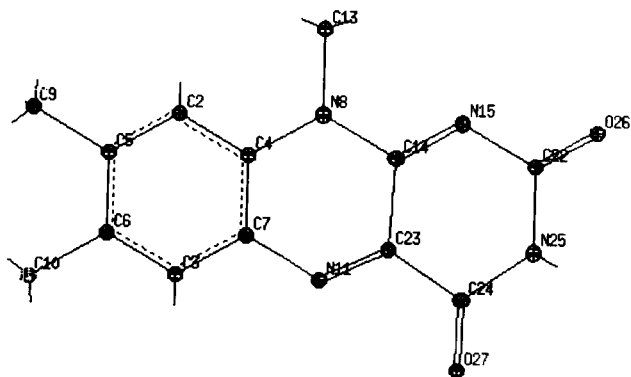


Figure 5: The Modified Version of the Flavin Within the Protein Environment Used in the Spartan Program

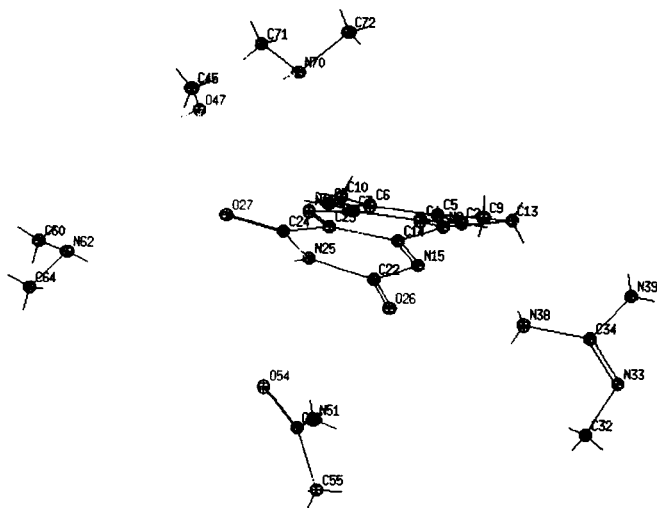


Figure 6: The Modified Version of the 8-Azido-FMN Used in the Spartan Program

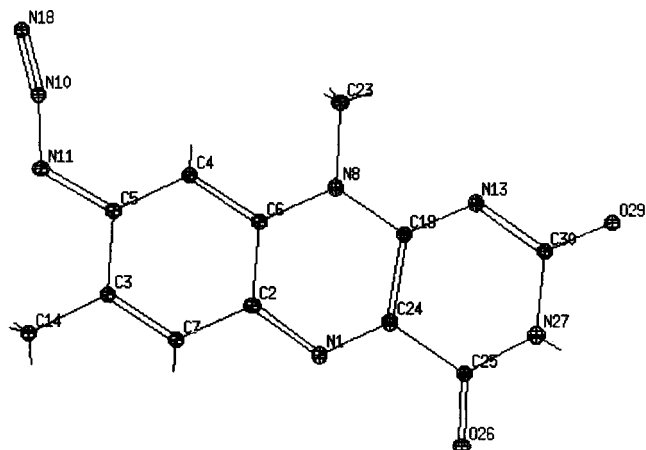


Figure 7: The Modified Version of the 6-Sulfoxo-FMN Used in the Spartan Program

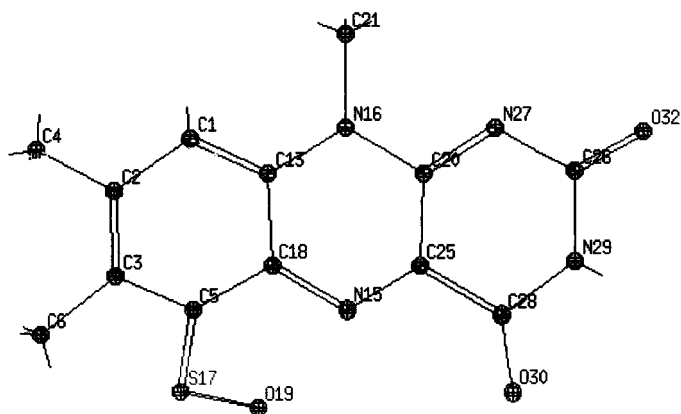


Figure 8: The Dipole Moment of the Modified FMN Outside and Inside the Protein Environment (Yellow Arrow is the Dipole Moment and Pink Lines are the Hydrogen Bonds)

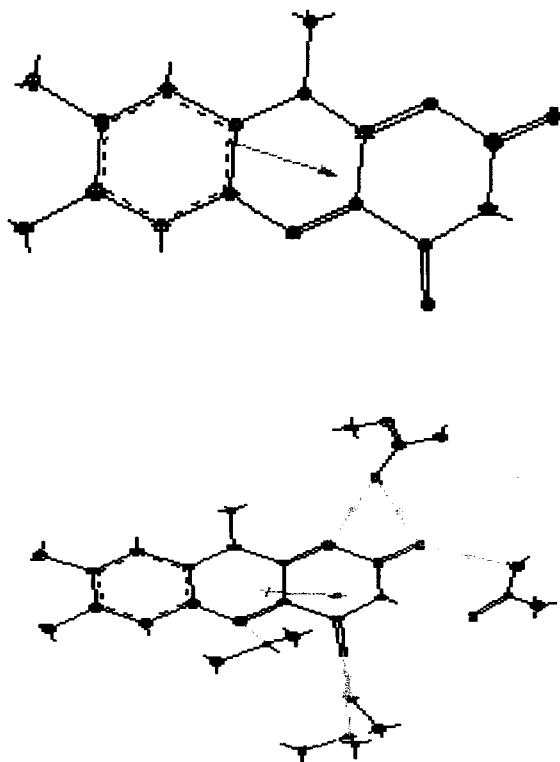


Figure 9: The Dipole Moment of the Modified 8-Azido-FMN Outside and Inside the Protein Environment (Yellow Arrow is the Dipole Moment and Pink Lines are the Hydrogen Bonds)

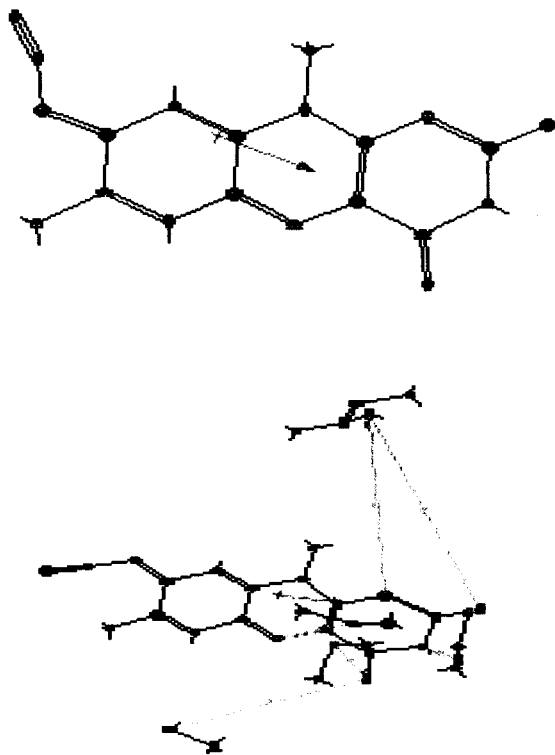


Figure 10: The Dipole Moment of the Modified 6-Sulfoxo-FMN Outside and Inside the Protein Environment (Yellow Arrow is the Dipole Moment and Pink Lines are the Hydrogen Bonds)

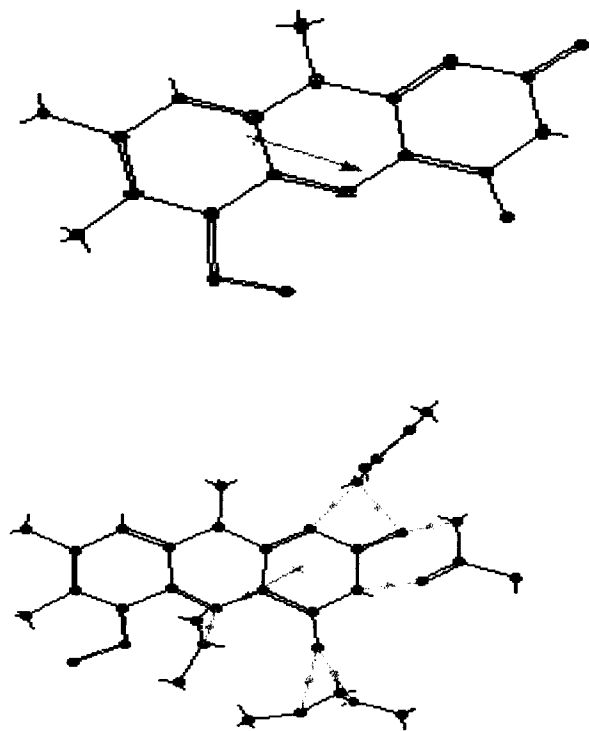


Figure 11: The Major Changes in the Electrostatic Charges for the FMN, 8-Azido-FMN, and 6-Sulfoxo-FMN With the Major Positive Changes Represented by Blue and the Major Negative Changes Represented by Red

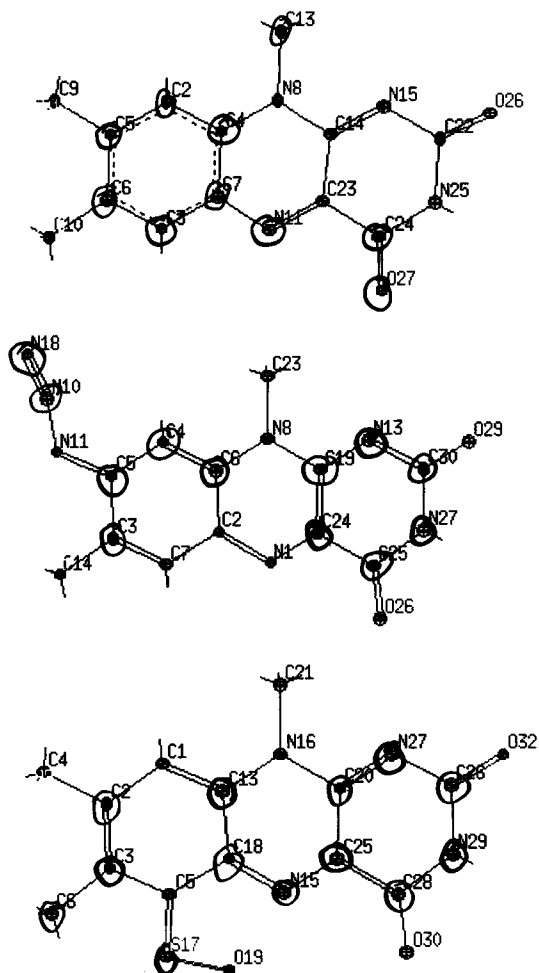
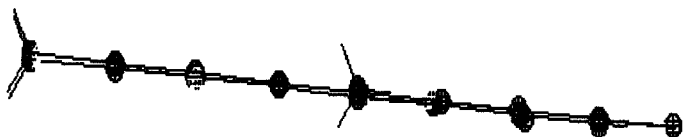


Figure 12: a) Flavin Without the Protein Environment Has a Planar Ring System
b) Flavin Within the Protein Environment Has a "Butterfly" Ring System

a)



b)

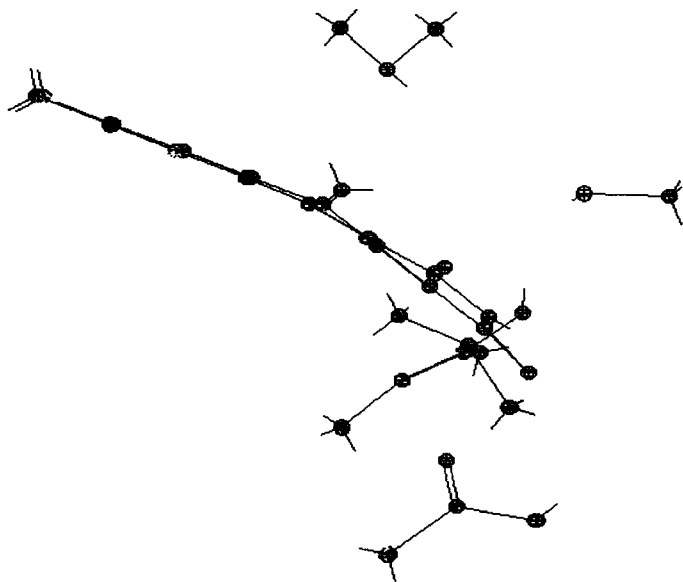


Figure 13: Some of the Possible Resonance Structures of FMN - The starred structures are the structures most likely formed in the stabilization of flavin within the protein environment.

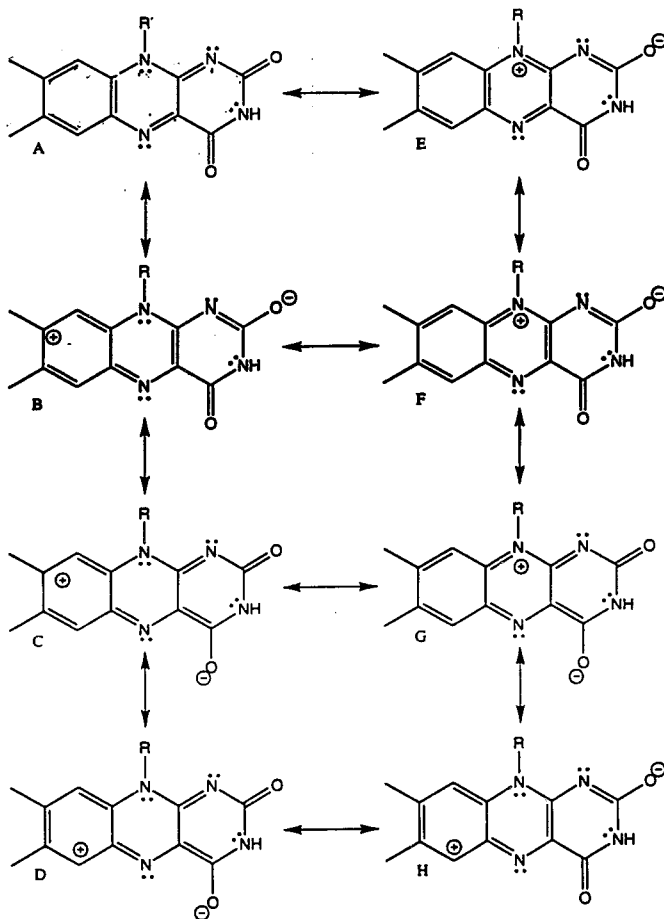


Figure 14: Two of the Possible Resonance Structures of 8-Azido-FMN

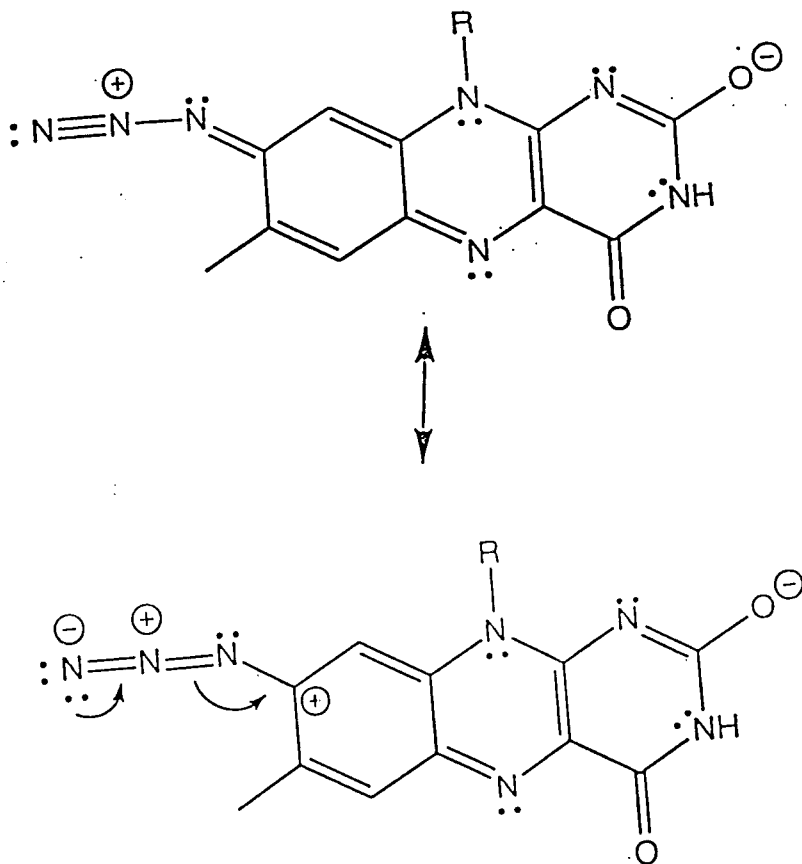
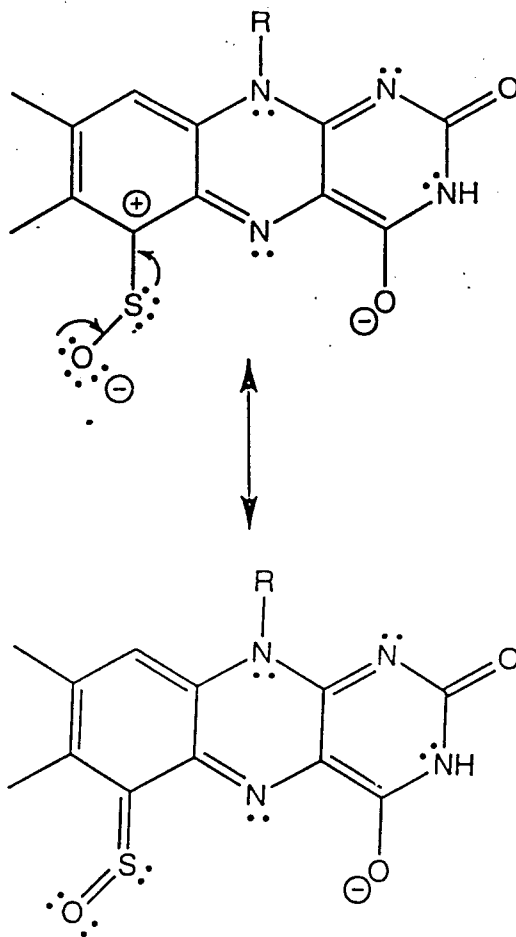


Figure 15: Two of the Possible Resonance Structures of 6-Sulfoxo-FMN



Work Cited:

- Abramovitz, Aaron S. & Massey, Vincent, Interaction of Phenols with Old Yellow Enzyme: Physical Evidence for Charge-Transfer Complexes, The Journal of Biological Chemistry, Volume 251, No. 17, September 10, 1976, p.5327-5336
- Abramovitz, Aaron S. & Massey, Vincent, Purification of Intact Old Yellow Enzyme Using an Affinity Matrix for the Sole Chromatographic Step, The Journal of Biological Chemistry, Volume 251, September 10, 1976, p. 5321-5326
- Fox, Kristin M. & Karplus, P. Andrew, Old Yellow Enzyme at 2 Å Resolution: Overall Structure, Ligand Binding, and Comparison With Related Flavoproteins, Section of Biochemistry, Molecular and Cell Biology, Cornell University, Ithaca, November 1994, p. 1089-1105
- Gatti Domenico L.; Palfey, Bruce A.; Soo Lah, Myoung; Entsch, Barrie; Massey, Vincent; Ballou, David P.; Ludwig, Martha L., The Mobile Flavin of 4-OH Benzoate Hydroxylase, Science, Volume 266, October 7, 1994, p. 110-4
- Ghisla, Sandro & Massey, Vincent, New Flavins for Old: Artificial Flavins as Active Site Probes of Flavoproteins, Biochemistry Journal, Volume 239, 1986, p.1-12
- Hill, Susan; Austin, Sara; Eydmann, Trevor; Jones, Tamera; Dixon, Ray; Azotobacter Vinelandii NIFL is a Flavoprotein that Modulates Transcriptional Activation of Nitrogen-Fixation Genes Via a Redox-Sensitive Switch, Volume 93, 1996, p. 2143-8
- Hyperchem Computational Chemistry Molecular Visualization and Simulation, Hypercube, Inc., Canada, August 1995, p. 275-7
- Merenyl, Gabor & Lind, Johan, Chemistry of Peroxidic Tetrahedral Intermediates of Flavin, Journal of American Chemical Society, Volume 113, 1991, p. 3146-3153
- Miller, Susan M., 2'-Fluoro-2'-deoxy-D-arabino flavin: Characterization of a Novel Flavin and Its Effects on the Formation and Stability of Two-Electron-Reduced Mercuric Ion Reductase, Biochemistry, Volume 34, 1995, p. 13066-73
- Moonen, Chrit J.; Vervoort, Jacques; Muller, Franz, Reinvestigation of the Structure of Oxidized and Reduced Flavin: Carbon-13 and Nitrogen-15 Nuclear Magnetic Resonance Study, Biochemistry, 1984, p. 4859-4867.
- Schopfer, Lawrence M. & Massey, Vincent, "A Study of Enzymes," Volume III, S.A. Kuby, Ed., CRC Press, 1991, p. 248-269
- Van den Berghe-Snorek, Sharon & Stankovich, Marian T., Thermodynamic Control of Electron Transfer of Flavoproteins by Substrate Binding, Journal of American Chemical Society, 1984, Volume 106, p. 3685-3687
- Watmough, Nicholas J.; Leohr, James P.; Drake, Steven K.; Frerman, Frank E., Tryptophan Fluorescence in Electron-Transfer Flavoprotein: Ubiquinone Oxidoreductase: Fluorescence Quenching by a Brominated Pseudosubstrate, Biochemistry, Volume 30, 1991, p. 1317-1323